Quantum capacitance mediated carbon nanotube optomechanics

Stefan Blien, Patrick Steger, Niklas Hüttner, Richard Graaf, and Andreas K. Hüttel*
Institute for Experimental and Applied Physics, University of Regensburg, 93040 Regensburg, Germany

Cavity optomechanics[1] allows the characterization of a vibration mode, its cooling and quantum manipulation using electromagnetic fields. Regarding nanomechanical[2,3] as well as electronic properties[4,5], single wall carbon nanotubes are a prototypical experimental system. At cryogenic temperatures, as high quality factor vibrational resonators, they display strong interaction between motion and single-electron tunneling[6,7]. However, small vibrational deflection and length have made their optomechanical coupling to microwave fields, as used in solid state cavity quantum electrodynamics or quantum information experiments, so far impossible. Here, we demonstrate large optomechanical coupling of a suspended carbon nanotube quantum dot and a microwave cavity, amplified by several orders of magnitude via the inherent nonlinearity of Coulomb blockade. From an optomechanically induced transparency (OMIT) experiment[8], we obtain an outstanding single photon coupling of up to $g_0 = 2\pi \cdot 88\,\mathrm{Hz}$. This indicates that normal mode splitting and full optomechanical control of the carbon nanotube vibration in the quantum limit[9] is reachable in the near future. A unique experimental system becomes accessible, where the nanomechanically active part directly incorporates a quantum-confined electron system[10]. Mechanical manipulation and characterization via the microwave field is complemented by the manifold physics of single electron devices. Applications of mechanical systems in the quantum limit range from ultraprecise sensors to quantum information processing[11–13] and signal processing in a wide frequency range. Based on our work, a carbon nanotube can become a "switchboard" for quantum states, potentially allowing quantum information transfer between spin, charge, vibration quantum, or cavity photon.

The technically challenging integration of suspended cabon nanotubes into complex qantum devices has recently made significant advances[14–18], as has also the integration of nanotube quantum dots into coplanar microwave cavities[19,20]. Our device, depicted in Figure 1a, combines a half-wavelength coplanar microwave cavity with a suspended carbon nanotube quantum dot. Near the coupling capacitor, the center conductor of the niobium-based cavity is connected to a thin gate electrode, buried between source and drain contacts of the carbon nanotube, see the sketch of Figure 1b. At the cavity center, i.e., the location of the voltage node of its fundamental mode, a bias connection allows additional application of a dc voltage V_g to the gate. The device is mounted at the base temperature stage ($T \simeq 10\,\mathrm{mK}$) of a dilution refrigerator; for details see the Supplementary Information, section III, and Supplementary Figure S-3.

At cryogenic temperatures, electronic transport through the carbon nanotube is dominated by Coulomb blockade, with the typical behaviour of a small band gap nanotube[4]. Near the electronic band gap, sharp Coulomb oscillations of conductance can be resolved; a detailed measurement is shown in Figure 1c. A well-known method to detect the transversal vibration resonance of a suspended nanotube quantum dot is to apply a rf signal and measure the time-averaged dc current[6,22,23]. On resonance, the oscillating geometric capacitance, effectively broadening the Coulomb oscillations, leads to an easily recognizable change in current. This was used to identify the transversal vibration resonances of the device; Figure 1d plots the resonance frequencies over a wide gate voltage range. Two coupled vibration modes are observed, one of which clearly displays electrostatic softening[24,25]. At low gate voltages, $|V_\mathrm{g}| \leq 1.5\,\mathrm{V}$, where subsequent experiments are carried out, the resonance which we will utilize in the following is at $\omega_\mathrm{m} \simeq 2\pi \cdot 502.5\,\mathrm{MHz}$, with typical quality factors around or exceeding $Q_\mathrm{m} \sim 10^4$.

The combined suspended nanotube – cavity device forms a dispersively coupled optomechanical system[1]. The cavity has a resonance frequency of $\omega_\mathrm{c} = 2\pi \cdot 5.74\,\mathrm{GHz}$ with a decay rate of $\kappa_\mathrm{c} = 2\pi \cdot 13\,\mathrm{MHz}$, dominated by internal losses. Nevertheless, due to the large mechanical resonance frequency ω_m of the carbon nanotube, the coupled system is far in the resolved sideband regime $\omega_\mathrm{m} \gg \kappa_\mathrm{c}$, the most promising parameter region for a large number of optomechanical protocols including ground state cooling and quantum control.

To probe for optomechanical coupling, we perform an optomechanically induced transparency (OMIT) type experiment[8], cf. Figures 2a and 2b: a strong, red-detuned drive field ($\omega_\mathrm{d} \simeq \omega_\mathrm{c} - \omega_\mathrm{m}$) pumps the microwave cavity; the transmission of a weak, superimposed probe signal ω_p near ω_c is detected. A distinct, sharp OMIT absorption feature within the transmission resonance of the cavity becomes visible in the measurements of Figures 2c-e. It occurs due to destructive interference of the probe field with optomechanically upconverted photons of the drive field, when the two-photon resonance condition $\omega_\mathrm{p} - \omega_\mathrm{d} = \omega_\mathrm{m}$ is fulfilled[8], and shifts in frequency as expected when ω_d is detuned from the precise red sideband condition, see Figures 2d,e. Fitting the OMIT feature allows to extract the optomechanical coupling parameter $g = \sqrt{n_\mathrm{c}}\,(\partial\omega_\mathrm{c}/\partial x)\,x_\mathrm{zpf}$, describing the cavity detuning per displacement of the mechanical harmonic oscillator[1,8], see the Supplementary Information for details. With a driven cavity photon occupation of $n_\mathrm{c} = 67500$, one obtains a single-photon coupling rate of up to $g_0 = g/\sqrt{n_\mathrm{c}} = 2\pi \cdot 88\,\mathrm{Hz}$.

This value of g_0 strongly exceeds expectations from the device geometry[26]. For a mechanical oscillator dispersively coupled to a coplanar waveguide resonator, the coupling is given by $g_0 = (\omega_\mathrm{c}/2C_\mathrm{c})(\partial C_\mathrm{c}/\partial x)x_\mathrm{zpf}$, where C_c is the total capacitance of the cavity, x is the mechanical displacement, and x_zpf the mechanical zero-point fluctuation length scale. Assuming a metallic wire over a metallic plane and inserting device parameters[26], the coupling calculated from the change in geo-

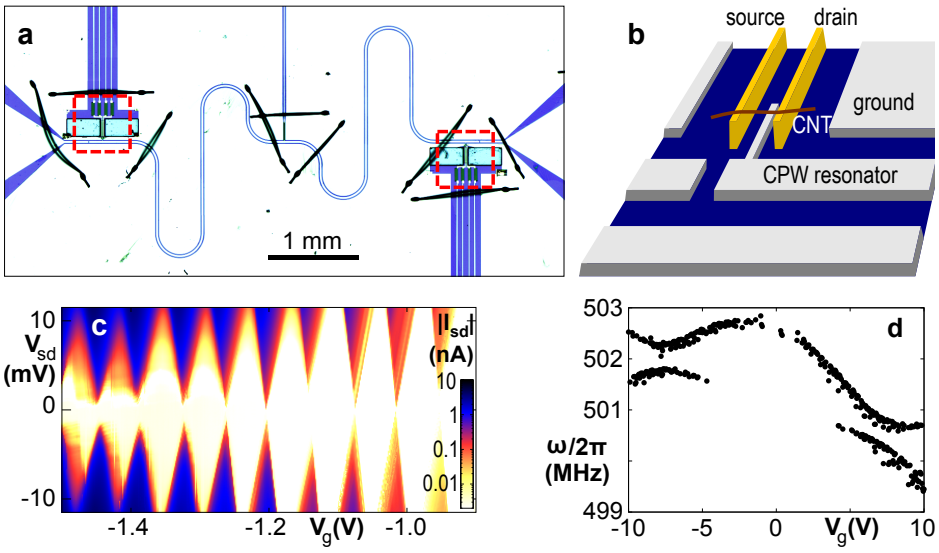

FIG. 1. **Integrating a suspended carbon nanotube quantum dot into a microwave cavity: a,** Optical micrograph showing a niobium-based $\lambda/2$ coplanar waveguide cavity for transmission measurement, with carbon nanotube deposition areas and dc contact structures (see the red dashed squares) near the coupling capacitors. For fabrication redundancy, two deposition areas exist on the device, but only one is used here. **b,** Simplified sketch of the nanotube deposition area, including source and drain and the buried gate connected to the cavity. **c,** dc transport characterization of the carbon nanotube quantum dot at $T_{\rm base} \simeq 10\,$mK, displaying the typical diamond-shaped Coulomb blockade regions of suppressed conductance[4,21]. **d,** Using rf excitation with an antenna and dc measurement[6,22], two transversal vibration modes can be traced across a large gate voltage range; the figure plots the detected resonance frequencies. The corresponding raw data can be found in the Supplementary Information, Figure S-5.

metric gate capacitance $C_g(x)$ becomes $\partial C_g/\partial x \sim 10^{-12}\,$F/m. This leads to $g_0^* = 2\pi \cdot 2.9\,$mHz, four orders of magnitude smaller than the measured g_0. To explain this discrepancy, we need to focus on the properties of the carbon nanotube as a quantum dot, with a strongly varying quantum capacitance $C_{\rm CNT}(x)$ as the displacement-dependent component of C_c dominating g_0.

Figure 2f depicts OMIT measurements for similar parameters as in Figures 2c-e, however, we now keep the drive frequency $\omega_{\rm d}$ constant and vary the gate voltage $V_{\rm g}$ across a Coulomb oscillation of conductance. The mechanical resonance frequency $\omega_{\rm m}$ shifts to lower frequencies in the vicinity of the charge degeneracy point. This electrostatic softening is a well-known characteristic of suspended carbon nanotube quantum dots[6,7]. More interestingly, the resulting gate-dependent coupling $g(V_{\rm g})$ (along with $g_0(V_{\rm g})$) is plotted in Figure 2g. It is maximal at the edges of the finite conductance peak, whereas at its center and on the outer edges, the coupling vanishes; the enhancement of g_0 is intrinsically related to Coulomb blockade.

Figure 3 explores the nature of this enhanced coupling mechanism. We assume a full separation of time scales $\omega_{\rm m} \ll \omega_{\rm c} \ll \Gamma$, where Γ describes the tunnel rates of the quantum dot. We can then define a generalized gate capacitance or quantum capacitance $C_{\rm CNT} = e\,\partial\langle N\rangle/\partial V_{\rm g}$, where $\langle N\rangle(V_{\rm g})$ is the number of charge carriers (here holes) on the quantum dot averaged over the tunneling events[27]. In a quantum dot, each Coulomb oscillation corresponds to the addition of one electron or hole on the quantum dot. The charge occupation $\langle N\rangle(V_{\rm g})$ resembles a step function, with the sharpness of the step given for zero bias voltage by lifetime and temperature broadening. This is plotted in Figure 3a, for the limit of $k_{\rm B}T \ll \Gamma$. The generalized capacitance $C_{\rm CNT}(V_{\rm g})$ becomes a Lorentzian, as plotted in Figure 3b.

Any motion δx modulates the *geometric* capacitance $C_{\rm g}(x)$. It thus shifts the position of the Coulomb oscillations in gate voltage, acting equivalent to an effective modulation of the gate voltage δV_g. With this, the optomechanical coupling g, scaling with $|\partial C_{\rm CNT}/\partial x|$, becomes proportional to the derivative $\partial C_{\rm CNT}/\partial V_{\rm g}$ and thus the second derivative of $\langle N\rangle(V_{\rm g})$, as is illustrated in Figure 3c. The resulting three key situations are sketched in Figures 3d-f: away from the conductance peak, the charge on the nanotube is constant, and only geometric capacitances change, see Figure 3d. On the flank of the conductance resonance, a small change δx ($\propto \delta C_g$) strongly modulates $C_{\rm CNT}$, see Figure 3e. At the center of the conductance resonance, the charge adapts to x, but the derivative $\partial C_{\rm CNT}/\partial V_{\rm g}$ and with it $g \propto |\partial C_{\rm CNT}/\partial x|$ is approximately zero.

The detailed derivation and the full expressions and values for Figure 3 can be found in the Supplementary Information, section IX, and in Supplementary Table S-I. We obtain an enhancement of the optomechanical coupling by a factor of $\sim 10^4$, with the broadening Γ of the Coulomb oscillation as dominating parameter. The experimental gate voltage dependence $g_0(V_{\rm g})$ is qualitatively reproduced very well. To obtain the quantitative agreement of Figure 3c, we have introduced a scaling prefactor as free fit parameter, resulting in

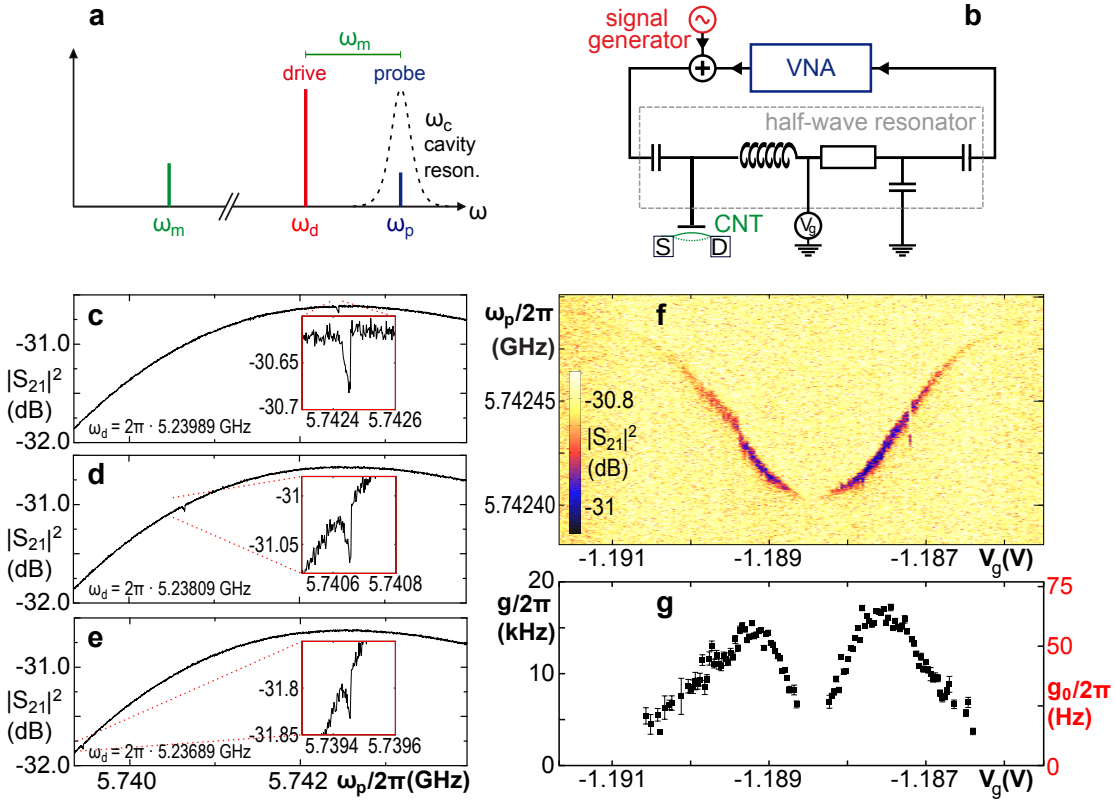

FIG. 2. **Optomechanically induced transparency (OMIT) in the Coulomb blockade regime: a,** Frequency scheme and **b,** detection setup of an OMIT measurement. A drive signal at $\omega_\mathrm{d} = \omega_\mathrm{c} - \omega_\mathrm{m}$ pumps the microwave cavity; the cavity transmission near the cavity resonance ω_c is characterized using a superimposed weak probe signal ω_p. Device parameters: $\omega_\mathrm{c} = 2\pi \cdot 5.74\,\mathrm{GHz}$, $\kappa_\mathrm{c} = 2\pi \cdot 13\,\mathrm{MHz}$, $\omega_\mathrm{m} \simeq 2\pi \cdot 502.5\,\mathrm{MHz}$. **c, d, e,** Probe signal transmission $\left|S_{21}(\omega_\mathrm{p})\right|^2$ for three different choices of ω_d, at $\omega_\mathrm{d} = \omega_\mathrm{c} - \omega_\mathrm{m}$ (**c**) and slightly detuned (**d, e**). The gate voltage $V_\mathrm{g} = -1.1855\,\mathrm{V}$ is fixed on the flank of a sharp Coulomb oscillation of conductance; $V_\mathrm{sd} = 0$. **f,** Probe signal transmission as in **c, d, e**, now for fixed $\omega_\mathrm{d} = 2\pi \cdot 5.23989\,\mathrm{GHz}$ and varied gate voltage V_g across a Coulomb oscillation. The depth of the OMIT feature allows evaluation of $g(V_\mathrm{g})$. **g,** Optomechanical coupling $g(V_\mathrm{g})$ (left axis) and corresponding single photon coupling $g_0(V_\mathrm{g}) = g(V_\mathrm{g})/\sqrt{n_\mathrm{c}}$ (right axis), extracted from the data of **f**; $n_\mathrm{c} = 67500$. Error bars indicate the standard error of the fit result.

$g_0^{\mathrm{exp}}/g_0^{\mathrm{th}} = 1.11$. Given the uncertainties of input parameters, this is an excellent agreement; see the Supplementary Information, section X, for a discussion of error sources.

In literature, many approaches have been pursued to enhance optomechanical coupling[12,13,27–34]. Resonant coupling, with $\omega_\mathrm{m} = \omega_\mathrm{c}$, has been demonstrated successfully for a carbon nanotube quantum dot[27], but does not provide access to the wide set of experimental protocols developed for the usual case of dispersive coupling and the "good cavity limit" $\omega_\mathrm{m} \gg \kappa_\mathrm{c}$. The mechanism presented here is most closely related to those where a superconducting charge qubit was coherently introduced between mechanical resonator and cavity[12]. However, the impact of single electron tunneling and shot noise on the optomechanical system shall require careful analysis.

Given the sizeable coupling in the good cavity limit $\kappa_\mathrm{c} \ll \omega_\mathrm{m}$, many experimental techniques for future experiments are at hand. First steps are demonstrated in Figure 4 in a two-tone spectroscopy experiment: a mechanical drive signal ω_a is applied simultaneously to a cavity pump signal at $\omega_\mathrm{d} = \omega_\mathrm{c} - \omega_\mathrm{a}$; the plotted cavity output power at ω_c clearly shows the optmechanical upconversion (Anti-Stokes scattering) at mechanical resonance $\omega_\mathrm{a} = \omega_\mathrm{m}$. In Figure 4a, the dc bias across the nanotube is set to zero, and the antenna drive kept at a minimum. In Figure 4b, both antenna drive and bias voltage have been increased. A background signal independent of device parameters emerges; at the same time, the upconverted signal displays a phase shift and destructive interference with the background for parts of the gate voltage range, meriting further measurements and analysis.

Future improvements of the optomechanical coupling via drive power and device geometry and of the detection sensitivity via the output amplifier chain shall allow detection of the thermal motion of the carbon nanotube and subsequently motion amplitude calibration. With this, a wide range of physical phenomena becomes experimentally accessible, ranging from side-band cooling of the vibration mode and potentially its quantum control[35] all the way to real-time observation of its interaction with single electron tunneling phenomena[36].

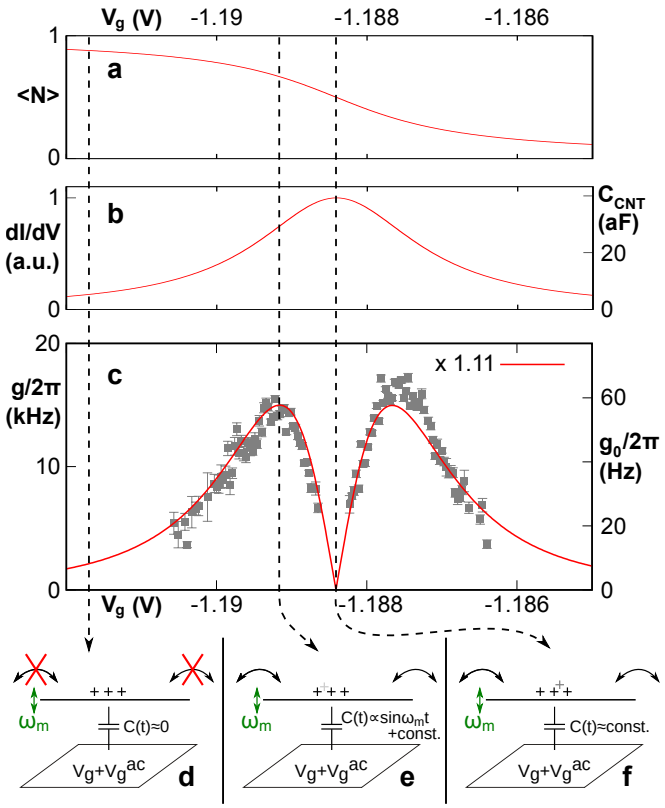

FIG. 3. **Coulomb blockade enhanced optomechanical coupling mechanism:** Solid lines correspond to the model of a Lorentz-broadened quantum dot level at $k_B T \ll \Gamma$. **a,** Time-averaged charge occupation $\langle N \rangle (V_g)$ of the quantum dot (note that we are in the hole conduction regime). **b,** Conductance $dI/dV_{sd}(V_g)$ (left axis) and generalized capacitance $C_{CNT} = e\,\partial\langle N\rangle/\partial V_g$ (right axis). **c,** Coulomb-blockade enhanced optomechanical coupling $g(V_g)$ (left axis) and single photon coupling $g_0(V_g)$ (right axis). The data points are identical to Figure 2g; the calculation result has been scaled with 1.11 to fit the data. **d-f,** Schemata for the situations corresponding to the dashed lines in **a-c**, see the text.

ACKNOWLEDGMENTS

The authors acknowledge funding by the Deutsche Forschungsgemeinschaft via Emmy Noether grant Hu 1808/1, SFB 631, SFB 689, SFB 1277, and GRK 1570. We would like to thank G. Rastelli, F. Marquardt, E. A. Laird, and Y. M. Blanter for insightful discussions, and Ch. Strunk and D. Weiss for the use of experimental facilities. The data has been recorded using Lab::Measurement[37].

AUTHOR CONTRIBUTIONS

A. K. H. and S. B. conceived and designed the experiment. P. S. and R. G. developed and performed nanotube growth and transfer; N. H. and S. B. developed and fabricated the coplanar waveguide device. The low temperature measurements were performed jointly by all authors. Data evaluation and writing of the manuscript was done jointly by S. B., N. H., and A. K. H. The project was supervised by A. K. H.

DATA AVAILABILITY

The datasets generated during and/or analysed during this study are available from the corresponding author on reasonable request.

SUPPLEMENTARY INFORMATION

See the Supplementary Information, which includes Refs. 1, 6, 8, 18, 22, 23, 26, 27, 38–46, for further information on device fabrication, measurement setup, the cavity photon number calibration, the used models, a parameter comparison with other optomechanical devices, and a discussion of error sources.

* andreas.huettel@ur.de

1 Aspelmeyer, M., Kippenberg, T. J. & Marquardt, F. Cavity optomechanics. *Rev. Mod. Phys.* **86**, 1391–1452 (2014).

2 White, C. T. & Todorov, T. N. Carbon nanotubes as long ballistic conductors. *Nature* **393**, 240 (1998).

3 Sazonova, V. *et al.* A tunable carbon nanotube electromechanical oscillator. *Nature* **431**, 284 (2004).

4 Laird, E. A. *et al.* Quantum transport in carbon nanotubes. *Rev. Mod. Phys.* **87**, 703 (2015).

5 Margańska, M. *et al.* Shaping electron wave functions in a carbon nanotube with a parallel magnetic field. *Phys. Rev. Lett.* **122**, 086802 (2019).

6 Steele, G. A. *et al.* Strong coupling between single-electron tunneling and nanomechanical motion. *Science* **325**, 1103 (2009).

7 Lassagne, B., Tarakanov, Y., Kinaret, J., Garcia-Sanchez, D. & Bachtold, A. Coupling mechanics to charge transport in carbon nanotube mechanical resonators. *Science* **325**, 1107–1110 (2009).

8 Weis, S. *et al.* Optomechanically induced transparency. *Science* **330**, 1520–1523 (2010).

9 Poot, M. & van der Zant, H. S. J. Mechanical systems in the quantum regime. *Physics Reports* **511**, 273 – 335 (2012).

10 Weig, E. M. *et al.* Single-electron-phonon interaction in a suspended quantum dot phonon cavity. *Phys. Rev. Lett.* **92**, 046804 (2004).

11 Rips, S. & Hartmann, M. J. Quantum information processing with nanomechanical qubits. *Phys. Rev. Lett.* **110**, 120503 (2013).

12 Pirkkalainen, J.-M. *et al.* Hybrid circuit cavity quantum electrodynamics with a micromechanical resonator. *Nature* **494**, 211 (2013).

13 Abdi, M., Pernpeintner, M., Gross, R., Huebl, H. & Hartmann, M. J. Quantum state engineering with circuit electromechanical three-body interactions. *Phys. Rev. Lett.* **114**, 173602 (2015).

14 Wu, C. C., Liu, C. H. & Zhong, Z. One-step direct transfer of pristine single-walled carbon nanotubes for functional nanoelec-

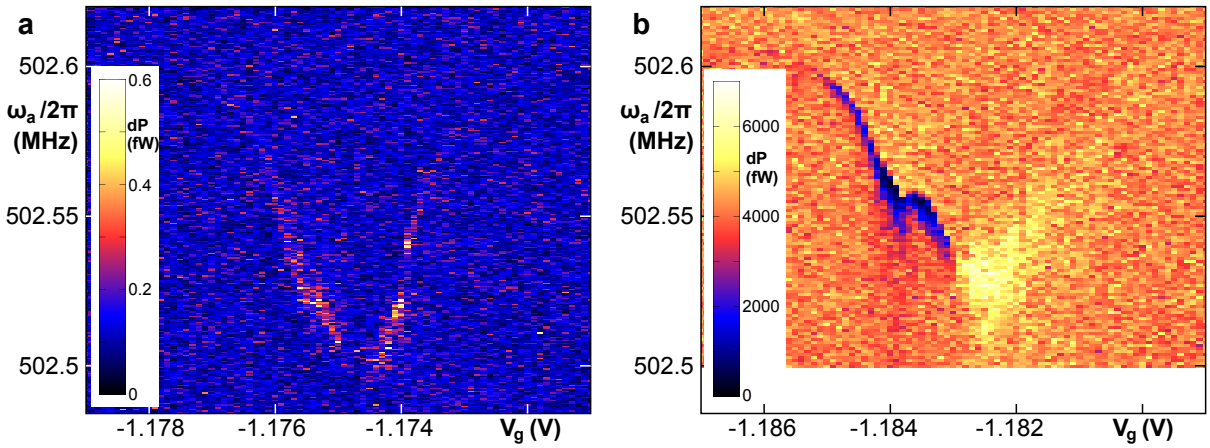

FIG. 4. **Two-tone spectroscopy:** Via an antenna, the carbon nanotube is driven at ω_a close its mechanical eigenfrequency; the microwave cavity is simultaneously pumped at $\omega_d = \omega_c - \omega_a$. The plots show the power output of the cavity at the upconverted frequency ω_c, with the nanotube acting as nonlinear element. Drive power $P_d = 20\,\mathrm{dBm}$ ($n_c \simeq 2.1 \times 10^4$), measurement bandwidth 5 Hz. **a,** Antenna generator power $P_a = -55\,\mathrm{dBm}$, bias $V_{sd} = 0$; **b,** antenna generator power $P_a = -30\,\mathrm{dBm}$, bias $V_{sd} = 0.5\,\mathrm{mV}$.

tronics. *Nano Letters* **10**, 1032–1036 (2010).

[15] Pei, F., Laird, E. A., Steele, G. A. & Kouwenhoven, L. P. Valley-spin blockade and spin resonance in carbon nanotubes. *Nature Nanotechnology* **7**, 630 (2012).

[16] Ranjan, V. *et al.* Clean carbon nanotubes coupled to superconducting impedance-matching circuits. *Nature Communications* **6**, 7165 (2015).

[17] Waissman, J. *et al.* Realization of pristine and locally tunable one-dimensional electron systems in carbon nanotubes. *Nature Nanotechnology* **8**, 569 (2013).

[18] Blien, S., Steger, P., Albang, A., Paradiso, N. & Hüttel, A. K. Quartz tuning-fork based carbon nanotube transfer into quantum device geometries. *Phys. Stat. Sol. B* **255**, 1800118 (2018).

[19] Delbecq, M. R. *et al.* Photon-mediated interaction between distant quantum dot circuits. *Nature Communications* **4**, 1400 (2013).

[20] Viennot, J. J., Dartiailh, M. C., Cottet, A. & Kontos, T. Coherent coupling of a single spin to microwave cavity photons. *Science* **349**, 408–411 (2015).

[21] Kouwenhoven, L. P. *et al.* *Electron transport in quantum dots* (Kluwer, 1997).

[22] Hüttel, A. K. *et al.* Carbon nanotubes as ultra-high quality factor mechanical resonators. *Nano Letters* **9**, 2547 (2009).

[23] Götz, K. J. G. *et al.* Nanomechanical characterization of the Kondo charge dynamics in a carbon nanotube. *Phys. Rev. Lett.* **120**, 246802 (2018).

[24] Wu, C. C. & Zhong, Z. Capacitive spring softening in single-walled carbon nanotube nanoelectromechanical resonators. *Nano Letters* **11**, 1448–1451 (2011).

[25] Stiller, P. L., Kugler, S., Schmid, D. R., Strunk, C. & Hüttel, A. K. Negative frequency tuning of a carbon nanotube nano-electromechanical resonator under tension. *Phys. Stat. Sol. B* **250**, 2518–2522 (2013).

[26] Regal, C. A., Teufel, J. D. & Lehnert, K. W. Measuring nanomechanical motion with a microwave cavity interferometer. *Nature Physics* **4**, 555 (2008).

[27] Ares, N. *et al.* Resonant optomechanics with a vibrating carbon nanotube and a radio-frequency cavity. *Phys. Rev. Lett.* **117**, 170801 (2016).

[28] Rimberg, A. J., Blencowe, M. P., Armour, A. D. & Nation, P. D. A cavity-Cooper pair transistor scheme for investigating quantum optomechanics in the ultra-strong coupling regime. *New J. Phys.* **16**, 055008 (2014).

[29] Heikkilä, T. T., Massel, F., Tuorila, J., Khan, R. & Sillanpää, M. A. Enhancing optomechanical coupling via the Josephson effect. *Phys. Rev. Lett.* **112**, 203603 (2014).

[30] Lecocq, F., Teufel, J. D., Aumentado, J. & Simmonds, R. W. Resolving the vacuum fluctuations of an optomechanical system using an artificial atom. *Nature Physics* **11**, 635 (2015).

[31] Pirkkalainen, J.-M. *et al.* Cavity optomechanics mediated by a quantum two-level system. *Nature Communications* **6**, 6981 (2015).

[32] Xue, Z.-Y., Yang, L.-N. & Zhou, J. Circuit electromechanics with single photon strong coupling. *Applied Physics Letters* **107**, 023102 (2015).

[33] Santos, J. T., Li, J., Ilves, J., Ockeloen-Korppi, C. F. & Sillanpää, M. Optomechanical measurement of a millimeter-sized mechanical oscillator approaching the quantum ground state. *New J. Phys.* **19**, 103014 (2017).

[34] Shevchuk, O., Steele, G. A. & Blanter, Y. M. Strong and tunable couplings in flux-mediated optomechanics. *Phys. Rev. B* **96**, 014508 (2017).

[35] O'Connell, A. D. *et al.* Quantum ground state and single-phonon control of a mechanical resonator. *Nature* **464**, 697 (2010).

[36] Barnard, A. W., Zhang, M., Wiederhecker, G. S., Lipson, M. & McEuen, P. L. Real-time vibrations of a carbon nanotube. *Nature* (2019).

[37] Reinhardt, S. *et al.* Lab::Measurement — a portable and extensible framework for controlling lab equipment and conducting measurements. *Computer Physics Communications* **234**, 216 (2019).

[38] Yuan, D. *et al.* Horizontally aligned single-walled carbon nanotube on quartz from a large variety of metal catalysts. *Nano Letters* **8**, 2576–2579 (2008).

[39] Kumar, M. & Ando, Y. Chemical vapor deposition of carbon nanotubes: a review on growth mechanism and mass production. *Journal of Nanoscience and Nanotechnology* **10**, 3739–3758 (2010).

[40] Schmid, D. R., Stiller, P. L., Strunk, C. & Hüttel, A. K. Magnetic damping of a carbon nanotube nano-electromechanical resonator.

New J. Phys. **14**, 083024 (2012).

[41] Simons, R. N. *Coplanar Waveguide Circuits, Components, and Systems* (John Wiley & Sons, Inc., 2001).

[42] Göppl, M. *et al.* Coplanar waveguide resonators for circuit quantum electrodynamics. *Journal of Applied Physics* **104**, 113904 (2008).

[43] Petersan, P. J. & Anlage, S. M. Measurement of resonant frequency and quality factor of microwave resonators: Comparison of methods. *Journal of Applied Physics* **84**, 3392–3402 (1998).

[44] Brydson, J. A. *Plastics Materials* (Butterworth-Heinemann, 1999), 7th edn.

[45] Singh, V. *et al.* Optomechanical coupling between a multilayer graphene mechanical resonator and a superconducting microwave cavity. *Nature Nanotechnology* **9**, 820 (2014).

[46] Wen, Y., Ares, N., Pei, T., Briggs, G. A. D. & Laird, E. A. Measuring carbon nanotube vibrations using a single-electron transistor as a fast linear amplifier. *Applied Physics Letters* **113**, 153101 (2018).